HHS Public Access

Author manuscript

Cancer Gene Ther. Author manuscript; available in PMC 2015 October 03.

Published in final edited form as:

Cancer Gene Ther. 2015 March ; 22(4): 215–221. doi:10.1038/cgt.2015.14.

Adenoviral-Mediated Imaging of Gene Transfer Using a Somatostatin Receptor-Cytosine Deaminase Fusion Protein

Kimberly A. Lears, M.S.[1], **Jesse J. Parry, B.S.**[1], **Rebecca Andrews, B.S.**[1], **Kim Nguyen, Ph.D.**[1], **Thaddeus J. Wadas, Ph.D.**[2,3], and **Buck E. Rogers, Ph.D.**[1,2]

[1]Department of Radiation Oncology, Washington University School of Medicine, St. Louis, MOf

[2]Mallinckrodt Institute of Radiology, Washington University School of Medicine, St. Louis, MOf

Abstract

Suicide gene therapy is a process by which cells are administered a gene that encodes a protein capable of converting a nontoxic prodrug into an active toxin. Cytosine deaminase (CD) has been widely investigated as a means of suicide gene therapy due to the enzyme's ability to convert the prodrug 5-fluorocytosine (5-FC) into the toxic compound 5-fluorouracil (5-FU). However, the extent of gene transfer is a limiting factor in predicting therapeutic outcome. The ability to monitor gene transfer, non-invasively, would strengthen the efficiency of therapy. In this regard, we have constructed and evaluated a replication-deficient adenovirus (Ad) containing the human somatostatin receptor subtype 2 (SSTR2) fused with a C-terminal yeast CD gene for the non-invasive monitoring of gene transfer and therapy. The resulting Ad (AdSSTR2-yCD) was evaluated *in vitro* in breast cancer cells to determine the function of the fusion protein. These studies demonstrated that the both the SSTR2 and yCD were functional in binding assays, conversion assays, and cytotoxicity assays. *In vivo* studies similarly demonstrated the functionality using conversion assays, biodistribution studies, and small animal positron-emission tomography (PET) imaging studies. In conclusion, the fusion protein has been validated as useful for the non-invasive imaging of yCD expression and will be evaluated in the future for monitoring yCD-based therapy.

Keywords

somatostatin receptor; cytosine deaminase; PET imaging

INTRODUCTION

In the past two decades, gene therapy has been developed as a promising approach to combat a variety of diseases. Over this time period, more than 1700 clinical gene therapy

Requests for reprints: Buck E. Rogers, Department of Radiation Oncology, Washington University School of Medicine, 4511 Forest Park Blvd. Suite 411, St. Louis, MO 63108. Phone: 314-362-9787; Fax: 314-362-9790; rogers@radonc.wustl.edu.

[3]Current Address: Department of Cancer Biology, Wake Forest University, Winston-Salem, NC

CONFLICT OF INTEREST

The authors declare no conflict of interest.

trials were conducted, with 65% addressing cancer (The Journal of Gene Medicine website, www.wiley.com/legacy/wileychi/genmed/clinical). Thus far, adenoviral vectors have been used in 24% of clinical trials, followed by retroviral vectors (21%) and naked/plasmid DNA (19%). Adenoviral vector-based approaches for cancer gene therapy have included: mutation compensation, genetic immunopotentiation, and molecular chemotherapy.[1] For mutation compensation, the molecular lesions in the cancer cell that are responsible for malignant transformation are corrected through gene transfer, while for genetic immunopotentiation, active immunization against tumor associated antigens is attempted. Molecular chemotherapy (also termed gene-directed enzyme prodrug therapy (GDEPT) or suicide gene therapy) is an approach for generating higher tumor concentrations of a cytotoxic drug than can normally be achieved through standard chemotherapy.[1] There are many genes that can be used for this approach, but two of the most common for this strategy are those encoding the herpes simplex virus type-1 thymidine kinase (HSV1-TK) and cytosine deaminase (CD). CD is an enzyme that can convert 5-fluorocytosine (5-FC) into the chemotherapy agent, 5-fluorouracil (5-FU). In this study, we chose to work with the CD system because, unlike with HSV1-TK, 5-FU is able to diffuse across the cell membrane into neighboring cells without the need for gap junctions, which results in a more powerful bystander effect.[2, 3]

Adenoviral-mediated delivery of CD has demonstrated success in animal models for treating several types of cancer including glioblastoma multiforme, colon, prostate, and breast either alone or in combination with radiation therapy.[4–11] In this regard, both the bacterial CD (bCD) and yeast CD (yCD) enzymes have been utilized. The yCD has been shown to have a K_m that is 22-fold lower than bCD for 5-FC, but is also more thermolabile than bCD, which may impact gene therapy strategies.[6] Subsequent engineering of both bCD and yCD have increased their efficacy by increasing their efficiency for 5-FC conversion and their thermostability, respectively.[5, 12–14] One issue that has limited the efficacy of this approach is the inability to determine the efficiency of CD gene transfer using non-invasive methods. In this regard, we have previously utilized the human somatostatin receptor subtype 2 (SSTR2) for imaging of gene transfer using gamma camera imaging and PET imaging.[15–19] Somatostatin receptors are members of the G protein-coupled receptor (GPCR) family that have seven transmembrane domains consisting of three extracellular loops, termed E1, E2, and E3.[18] SSTR2 is expressed on brain, spleen, and kidney tissues and overexpressed in a variety of tumor types, leading to the development of tumor imaging agents.[20] Therefore, we chose to develop a novel fusion protein consisting of yCD and SSTR2 that can be used to monitor the location, magnitude, and change in magnitude over time of CD using positron-emission tomographic (PET) imaging.

In this study, we describe the construction and characterization of a novel yCD fusion protein that consists of yCD linked to the C-terminus of the human somatostatin receptor subtype 2 (SSTR2) to create SSTR2-yCD. This initial study uses a non-replicative adenoviral vector as a model gene delivery vehicle to evaluate SSTR2-yCD *in vitro* and *in vivo*. An adenovirus containing the SSTR2-yCD was produced and evaluated for SSTR2 function using a radioligand binding assay and for yCD function using cytoxicity and 5-FC conversion assays in infected breast cancer cells. *In vivo* assays in human breast cancer xenografts injected with AdSSTR2-yCD showed conversion of 5-FC to 5-FU as well as

specific uptake of a PET ligand in biodistribution and small animal PET imaging. These results demonstrated that both the SSTR2 and yCD components of the fusion protein are functional and that this imaging approach should be useful for improving the efficacy of yCD-based therapy.

MATERIALS AND METHODS

Cell Lines and Construction of AdSSTR2-yCD

Human breast adenocarcinoma MCF-7 and T-47D cells were obtained from the American Type Culture Collection (ATCC, Manassas, VA), and both cell lines were maintained in DMEM (Life Technologies, Grand Island, NY) plus 10 mM HEPES (Mediatech, Herndon, VA) and 10% heat-inactivated fetal bovine serum (Sigma-Aldrich, St. Louis, MO). The yCD coding sequence was fused to the C-terminal end of human SSTR2 via a seven amino acid linker in an overlap extension polymerase chain reaction. The resulting product was cloned into pShuttle-CMV (Agilent Technologies, Santa Clara, CA) via XhoI and EcoRV, sites for which were incorporated into the construct via two primers for the PCR, and the resulting plasmid was pS-SSTR2-yCD. The clone was sequence verified to show the absence of mutations. Both the SSTR2 and yCD portions of the fusion were then validated in functional assays in transiently transfected MCF-7 and T-47D cells. Following the validation, pS-SSTR2-yCD was used to produce recombinant adenoviral plasmid, which was then transfected into AD-293 cells (ATCC) for the production of crude SSTR2-yCD adenovirus, which was sent to Q-Biogene (Montreal, Canada) for the production of purified AdSSTR2-yCD. AdSSTR2 was produced as previously described.[21]

Competitive Binding Assay

The B_{max} values of AdSSTR2 and AdSSTR2-yCD-infected T-47D and MCF-7 cells were determined by using a competitive binding assay with ^{125}I-Tyr^{11}-Somatostatin-14 (PerkinElmer, Boston, MA). AdSSTR2 or AdSSTR2-yCD was administered to cells at a concentration of 10 or 100 plaque forming units (pfu) per cell, and membrane preparations were made as previously described.[22] Protein concentrations were determined using the Pierce Non-Reducing Agent Compatible Kit (Rockford, IL). The membrane preparations were diluted in binding buffer (50 mM Tris-Cl, pH 7.4, 5 mM $MgCl_2$, 0.1% (w/v) bovine serum albumin (BSA), 0.5 mg/mL aprotinin, 200 mg/mL bacitracin, 10 mg/mL leupeptin, 10 mg/mL pepstatin) to obtain a concentration of 25 μg per 100 μL. A 96-well Multiscreen Durapore filtration plate (Millipore, Bedford, MA) pretreated with 0.1% polyethyleneimine via vacuum manifold aspiration was then washed with 300 μL of wash buffer (10 mM HEPES, 1 mM EDTA, 5 mM $MgCl_2$, 0.1% BSA) before adding 100 μL of each membrane preparation in triplicate per concentration of blocking reagent. The wells were then washed three times with wash buffer. Various concentrations of Tyr^{11}-somatostatin-14 (Bachem, Torrance, CA) blocking reagent, ranging from 0.01–55 nM, were then added to the wells in triplicate in a volume of 10 μL for both AdSSTR2 and AdSSTR2-yCD membrane preparation. ^{125}I-Tyr^{11}-SST-14 ligand (PerkinElmer) was diluted in binding buffer to yield ~10,000 cpm per 100 μL, which was then added to each well. The blocking reagent and radioligand were incubated with shaking for one hour at room temperature. All wells were washed twice with wash buffer, and all remaining liquid was removed via vacuum manifold.

The membranes, once dry, were placed in individual tubes, and the bound radioactivity was determined using a Packard II gamma counter (PerkinElmer). The data was entered into GraphPad Prism 4 (La Jolla, CA) to generate homologous competitive binding curves using the one-site homologous competition with depletion equation, and B_{max} values were calculated from the curves.

In Vitro yCD Conversion Assay

The cytosine deaminase (CD) activity of AdSSTR2 and AdSSTR2-yCD-infected T-47D and MCF-7 cells was determined by performing ^{3}H-5-FC (Moravek Biochemicals, Brea, CA) conversion assays. AdSSTR2 or AdSSTR2-yCD were administered to cells at 10 or 100 pfu/cell, and 2 days later, the cells were scraped from their flasks using PBS/EDTA (PBS, 500 mM EDTA, 200 mM PMSF). Next, the cells were centrifuged for 10 minutes at 4,000 rpm at 4°C, the supernatant aspirated, and the cell pellet was frozen at −80°C overnight. The pellet was then resuspended in complete extraction buffer (50 mM Tris, pH 8.0, 23 mg/mL NaCl, 36 μg/mL EGTA, 5% v/v glycerol, 100 mM DTT, 200 mM PMSF) and incubated on ice for 15 minutes followed by centrifugation at 1,400 rpm for 5 minutes at 4°C. The supernatant was collected, and protein concentrations were determined using the Pierce Reducing Agent Compatible Kit. For each reaction, 4 μg of respective whole cell extract were combined with 3 μCi of ^{3}H-5-FC and H_2O to a total volume of 30 μL. The reactions were incubated in a 37°C water bath, and at various time points, an aliquot was removed, and the reaction stopped by adding 1 M Acetic Acid and a 4 mg/mL 5-Fluorocytosine/5-Fluorouracil mixture. The samples were spotted onto TLC plates (20 × 20 cm TLC plastic sheets, Silica gel 60 F_{254}) (EMD Chemicals, Darmstadt, Germany), and the plates were run in 86:14 butanol:water solvent. Once dry, 5-FC and 5-FU were identified using a handheld UV transilluminator at 254 nm, and strips of the TLC plates with each corresponding compound were placed into separate scintillation tubes with 5 mL EcoLume scintillation fluid (MP Biomedicals, Irvine, CA). The samples were then analyzed using a TriCarb Scintillation Counter (PerkinElmer) to determine the amount of 5-FC and 5-FU at each time point. The data was plotted as pmol of 5-FU formed over time, and CD activity was determined by dividing the slope of the curve by the amount of protein added.

In Vitro 5-Fluorocytosine Cytotoxicity Assay

IC_{50} (50% inhibitory concentration) values for AdSSTR2-yCD-infected MCF-7 cells were determined by using *in vitro* cytotoxicity assays. AdSSTR2 or AdSSTR2-yCD were administered to cells at 10 or 100 pfu/cell, and the cells were then plated into 96-well plates at a concentration of 5×10^{4} cells per well. After the cells had 1 day to adhere, the media was aspirated and replaced with various concentrations of 5-FC in cell culture media, ranging from 0–1000 μg/mL. After incubating at 37°C for 5 days, the media was aspirated, the wells were washed with PBS, and 100 μL of 2% crystal violet in 70% ethanol were added to each well. The plates were incubated at room temperature for 3h before removing the stain and washing the wells with H_2O. Once the wells were dry, the optical density was measured at 540 nm on a Thermo Multiskan MCC Photometer (Fisher Scientific, Houston, TX). Percent survival was determined by dividing the absorbance value of the wells with 5-FC by the absorbance of the wells without 5-FC. The data was entered into GraphPad Prism 4 to generate sigmoidal dose response curves, and IC_{50} values were calculated from the curves.

In Vivo yCD Conversion in Tumor Xenografts

All animal studies were performed in accordance with the guidelines for the care and use of research animals by the Washington University Animal Studies Committee. Six days prior to cell implantation, a 60-day release β-Estradiol pellet (Innovative Research of America, Sarasota, FL) was implanted into the left flank of each 4 week-old female Fox Chase C.B. 17-SCID mouse (Charles River Lab, Wilmington, MA). MCF-7 cells mixed 1:1 with Matrigel Basement Membrane Matrix (Becton Dickinson, Palo Alto, CA) were implanted at 1×10^7 cells per tumor in the right flank of each mouse. The tumors were allowed to grow for 5–6 weeks and were then injected with saline, AdSSTR2 at 3×10^9 plaque forming unit (pfu)/tumor, or AdSSTR2-yCD at 1×10^9 or 3×10^9 pfu/tumor. Tumors were dissected 48 hours later and were rinsed, weighed, and minced on ice. The tumors (250–450 mg) were then resuspended in 1 mL complete extraction buffer plus a Complete Protease Inhibitor tablet (Roche, Indianapolis, IN) and sonicated. After incubating on ice for 30 minutes, the extracts were centrifuged at 10,000 rpm for 20 minutes at 4°C. The supernatant was harvested and assayed for protein concentration, and yCD conversion assays were performed as described above.

Radiolabeling of CB-TE2A-Y3-TATE with ^{64}Cu

The peptides Y3-TATE and CB-TE2A-Y3-TATE were prepared by standard literature protocols.[23, 24] ^{64}Cu-CB-TE2A-Y3-TATE was prepared according to a literature procedure.[25] Briefly, the complexation of ^{64}Cu to CB-TE2A-Y3-TATE was achieved by reacting 1 μg (6.3×10^{-4} μmol) of CB-TE2A-Y3-TATE, 118 μL of 0.1 M NH_4OAc (pH = 8.0) and 37 MBq of $^{64}CuCl_2$ in 0.1N HCl for 1.5 h at 95°C. The reaction was further purified using a previously published method.[26] Purity after purification was greater than 95% based upon radio-TLC and radio-HPLC analysis. Specific Activity after purification was observed to be 39,900MBq/μmol (785 μCi/μg)

Biodistribution

β-Estradiol pellets and MCF-7 tumors were implanted and allowed to grow as above. The mice were anesthetized and intratumoral injections of AdSSTR2 (n=3) or AdSSTR2-yCD (n=3) (each at 3×10^9 pfu per tumor in a volume of 30 μL of sterile saline) were performed. Two days following the viral injections, tail vein injections of ^{64}Cu-CB-TE2A-Y3-TATE (185 kBq (5 μCi); 6 ng) were performed. Two other groups of animals served as negative controls, with mice receiving an intratumoral saline injection (n=3) and another group of animals receiving an intratumoral saline injection followed by a co-injection of ^{64}Cu-CB-TE2A-Y3-TATE and 200 μg of Y3-TATE to serve as a block (n=4). The mice were sacrificed 4 h after injection, and blood, liver, spleen, pancreas, adrenals, kidney, muscle, tumor, bone, and tail were removed. Tissue samples were weighed and placed in a gamma counter for determination of radioligand content. The percent injected dose per gram (% ID/g) was calculated based on a decay-corrected standard dose.

MicroPET/CT Imaging Studies

Mice were implanted with β-estradiol pellets on the rear flank and MCF-7tumors on the axillary thorax and allowed to grow as described above. The mice (n = 3) were injected

intratumorally with 3×10^9 pfu of AdSSTR2-yCD or with saline, followed by i.v. injection of ^{64}Cu-CB-TE2A-Y3-TATE two days later (4.1 MBq (110 μCi); 125 ng). One group of saline injected mice received a co-injection of ^{64}Cu-CB-TE2A-Y3-TATE and 200 μg of Y3-TATE to serve as a block. Four hours after injection, the mice were anesthetized with 1–2% isoflurane, positioned supine, and imaged on microPET FOCUS 220 or Inveon PET small animal scanners (Siemens Medical Solutions, Malvern, PA). The PET acquisition times were 10 min and CT images were obtained using a MicroCAT II System (ImTek, Inc., Knoxville, TN). The images were reconstructed with an Ordered-Subset Estimation Maximization (OSEM) algorithm which included corrections for scatter and attenuation. Regions of interest were drawn to encompass the entire tumor to determine the maximum activity concentration (nCi/cc) in the tumor. To calculate the standardized uptake values (SUVs), the nCi/cc was divided by the nCi injected (decay corrected to the scan start time) and multiplied by the mouse weight.

Statistical Analysis

All data are presented as the mean ± SEM. The Student's two-tailed *t*-test was used to determine statistical significance at the 95% confidence level, with $p \leq 0.05$ being considered significantly different.

RESULTS

Construction of AdSSTR2-yCD

Crude AdSSTR2-yCD was validated for SSTR2 function in a single-point binding assay, and the yCD portion of the fusion was validated in a single time point cytosine deaminase conversion assay. Following these validations, the crude virus was used to produce cesium chloride-purified AdSSTR2-yCD (Q-Biogene) at a titer of 3.25×10^{11} pfu/mL. The AdSSTR2 had a titer of 3.16×10^{11} pfu/mL.

Competitive Binding Assay

To demonstrate that the SSTR2 portion of the fusion protein was functional, a competitive binding assay was performed using cells infected with AdSSTR2-yCD at 10 and 100 plaque forming units (pfu) per cell. A representative curve of MCF-7 cells infected at 10 and 100 pfu/cell is shown in Figure 1. The MCF-7 and T-47D cells both showed high affinity binding of ^{125}I-Tyr^{11}-SST-14 with K_d's of ~50–200 pM at both 10 and 100 pfu/cell (Table 1). In addition, the expression levels were evaluated and MCF-7 cells had B_{max} values of 764 ± 132 and 1829 ± 293 fmol/mg after infection at 10 and 100 pfu/cell, respectively, while T-47D cells had B_{max} values of 40 ± 6 and 217 ± 25 fmol/mg, respectively. When compared to the previously utilized AdSSTR2, there were no significant differences in the K_d or in the B_{max} values at 10 and 100 pfu/cell. A binding assay on uninfected MCF-7 and T-47D cells did not show endogenous SSTR2 expression (data not shown). However, others have shown low levels of SSTR2 on T-47D cells[27], while there are conflicting reports about SSTR2 expression on MCF-7 cells.[28, 29]

In Vitro yCD Conversion Assay

The yCD conversion activity was determined by measuring the conversion of ^{3}H-5-FC to ^{3}H-5-FU in MCF-7 and T-47D cells infected with AdSSTR2-yCD at 10 and 100 pfu/cell. Table 2 shows the conversion results, in terms of pmol/min/mg. The MCF-7 cells infected at 100 pfu/cell showed the highest rate of conversion at 386 ± 27 compared to 214 ± 58 for T-47D cells infected at 100 pfu/cell. By comparison, when the cells were infected at 10 pfu/cell, the conversion rate was lower at 62 ± 11 and 11 ± 1 for MCF-7 and T-47D cells, respectively.

In Vitro 5-Fluorocytosine Cytotoxicity Assay

To determine the 5-FC sensitivity of MCF-7 cells to AdSSTR2-yCD mediated suicide gene expression, the cells were infected at 10 and 100 pfu/cell and treated with various concentrations of 5-FC, and the relative cell viability was determined using the crystal violet staining assay. Since the previous assays demonstrated that the MCF-7 cells were more susceptible to infection with AdSSTR2-yCD than the T-47D cells, only the MCF-7 cells were evaluated for this and future assays. A representative cytotoxicity curve is shown in Figure 2. This shows that the IC_{50} at 100 pfu/cell was 4.2 ± 1.4 μg/mL compared to 27.2 ± 10.7 μg/mL after infection at 10 pfu/cell. The IC_{50} was > 1000 μg/mL for cells infected with AdSSTR2 at either 10 or 100 pfu/cell (data not shown). Infection with AdSSTR2-yCD or AdSSTR2 at 10 and 100 pfu/cell (without addition of 5-FC) decreased cell viability by about 2% and 26%, respectively when compared to uninfected cells (data not shown).

In Vivo yCD Conversion in Tumor Xenografts

We next wanted to confirm that an intratumoral injection of AdSSTR2-yCD would result in functional yCD in mice bearing MCF-7 tumor xenografts. These results show that intratumoral injection of 1×10^{9} pfu of AdSSTR2-yCD resulted in a ^{3}H-5-FC conversion rate of 193 ± 41 pmol/min/mg compared to 698 ± 81 pmol/min/mg when 3×10^{9} pfu were injected (Table 2). In contrast, there was no detectable conversion when AdSSTR2 or saline were injected.

Biodistribution

The ability of AdSSTR2-yCD to induce expression of SSTR2-yCD after intratumoral injection into MCF-7 tumor xenografts was determined using a radioactive biodistribution study 4 h after i.v. injection of ^{64}Cu-CB-TE2A-Y3-TATE. The results are in Figure 3 and show that there was no significant difference in the tumor uptake of ^{64}Cu-CB-TE2A-Y3-TATE following injection of AdSSTR2-yCD (1.55 ± 0.11% ID/g) or AdSSTR2 (1.73 ± 0.14% ID/g). These values were not significantly greater than the control mice (1.04 ± 0.21% ID/g), but were significantly greater ($p < 0.01$) than the control + block mice (0.23 ± 0.03% ID/g). There were no significant differences between the two control groups except for the pancreas being higher in the control vs. control + block. The liver and spleen uptake of ^{64}Cu-CB-TE2A-Y3-TATE after intratumoral injection of AdSSTR2 was significantly greater ($p < 0.03$) than all of the other groups, while the liver uptake was significantly greater ($p < 0.01$) after injection of AdSSTR2-yCD compared to control, but did not reach significance when compared to control + block. Conversely, the spleen uptake after

AdSSTR2-yCD injection was significantly greater when compared to control + block ($p < 0.01$), but not when compared to control.

MicroPET/CT Imaging Studies

To test whether AdSSTR2-yCD could be used to image *in vivo* gene transfer, AdSSTR2-yCD was injected intratumorally into MCF-7 tumor xenografts followed by i.v. injection of ^{64}Cu-CB-TE2A-Y3-TATE. Small animal PET/CT images of ^{64}Cu-CB-TE2A-Y3-TATE at 4 h are shown in Figure 4. Coronal (**A,B**) and transaxial (**C,D**) views of two mice (one receiving AdSSTR2-yCD (**A,C**) and the other receiving saline (**B,D**)) from the fused PET/CT for mice bearing MCF-7 xenografts are shown in this figure. Tumor uptake is observed in the mice that received AdSSTR2-yCD, while mice that received the intratumoral saline did not show distinguishable uptake in the tumors. Clearance of ^{64}Cu-CB-TE2A-Y3-TATE is observed through the liver and kidneys, which match the biodistribution results. Figure 4E shows the SUV analysis from the PET/CT studies. This shows that the tumor uptake of ^{64}Cu-CB-TE2A-Y3-TATE was selective in tumors injected with AdSSTR2-yCD while retention was not observed in tumors injected with saline. Interestingly, there was no difference between the group that received saline and ^{64}Cu-CB-TE2A-Y3-TATE compared to the group that received saline and ^{64}Cu-CB-TE2A-Y3-TATE with the blocking agent as observed in the biodistriubtion study. The tumor uptake of ^{64}Cu-CB-TE2A-Y3-TATE was significantly greater ($p < 0.03$) when the tumors were injected with AdSSTR2-yCD compared to saline injection.

DISCUSSION

Gene-directed enzyme prodrug therapy using the CD/5-FC system has been investigated for some time.[1] It has been utilized as a stand-alone therapeutic approach and has been combined with other gene therapy, chemotherapy, and radiotherapy strategies.[30, 31] In addition, the efficacy of this GDEPT approach has been enhanced by creating uracil phophoribosyltransferase fusion genes with CD, thymidine kinase fusion genes with CD, or mutant bCD enzymes to increase the catalytic conversion of 5-FC to 5-FU.[5, 11, 12, 32, 33] However, one of the major limitations of adenoviral-based gene therapy in general, and specifically CD-based molecular chemotherapy, is the inability to determine the level of *in vivo* gene transfer non-invasively. Tissue biopsies to determine levels of gene transfer are not ideal because they are invasive, not easily repeated, and are subject to sample variability that does not give a global picture of gene transfer. Therefore, development of a CD construct that can be used to monitor the location, magnitude, and change in magnitude over time of gene transfer non-invasively would address this limitation.

Previously, several approaches have been investigated to non-invasively determine the expression of CD. One approach for monitoring CD enzyme activity has been through the use of ^{19}F magnetic resonance spectroscopy (MRS).[34–37] This approach has been used to demonstrate the conversion of 5-FC to 5-FU in animal models and to quantify their concentrations as well as their resulting metabolites.[35, 36] However, the sensitivity of MRS is inherently limited and sufficient metabolite concentrations must be sustained during image acquisition to achieve adequate resolution.[35] It has been suggested that 5-FC is not an

effective probe for MRS of CD because the metabolism of 5-FC by CD does not result in persistently elevated levels of fluorinated metabolites.[35, 36] Another approach has been through the use of nuclear imaging methods. This method has generally used a fusion protein consisting of HSV1-TK and CD with the main purpose of combining these prodrug strategies for increasing therapeutic efficacy.[38–41] However, HSV1-TK can also be used as a reporter gene that can be imaged with radioactive probes. These probes have consisted of uracil nucleoside derivatives radiolabeled with iodine isotopes for PET and single photon emission computed tomographic (SPECT) imaging or acycloguanosine derivatives radiolabeled with ^{18}F for PET imaging. These probes are transported into cells, phosphorylated by cells expressing HSV1-TK (or fusion protein), and the phosphorylated product is trapped, leading to a signal when compared to surrounding tissue not containing HSV1-TK. Hackman *et. al*. used ^{124}I-FIAU to image rats with tumor cells stably expressing the CD/TK fusion gene by PET.[40] Freytag *et. al.* used ^{18}F-FHBG to image CD/TK expression by PET in dogs that had been injected in the pancreas with a replicative Ad vector.[38] However, the correlation between HSV1-TK expression and the accumulation of radiolabeled probes when HSV1-TK is expressed at high levels is lacking.[38] Thus, the HSV1-TK reporter may not be appropriate for quantifying the expression level of CD in gene therapy protocols and another reporter may be necessary.

Our previous studies used the radiolabeled somatostatin analogs, ^{111}In-DTPA-octreotide (Octreoscan), ^{99m}Tc-P829 (NeoTect), ^{99m}Tc-P2045, or ^{94m}Tc-Demotate to demonstrate localization in a tumor injected directly with an adenovirus (AdSSTR2) encoding the SSTR2 gene driven by a cytomegalovirus (CMV) promoter. Importantly, we demonstrated that there is a strong correlation between the expression of SSTR2 and the tumor uptake of ^{99m}Tc-P2045 after intratumoral injection of various amounts of AdSSTR2.[42] Therefore, the focus of the present study was to construct and evaluate a novel fusion gene consisting of SSTR2 and CD.

In the present study, we constructed an adenoviral vector encoding for a fusion protein between SSTR2 and yCD and evaluated this construct (AdSSTR2-yCD) in human breast cancer cells. The *in vitro* binding studies demonstrated that SSTR2 was still functional as it bound somatostatin at an affinity of ~85–200 pM in both MCF-7 and T-47D cells. This was similar to when the wild-type receptor was utilized in these cells (~50–190 pM). As expected, an increase in receptor concentration (B_{max}) was observed when infecting at 100 pfu/cell compared to 10 pfu/cell. In addition, these studies showed that MCF-7 cells were more easily infected with adenovirus compared to the T-47D cells as determined by the higher expression observed in the MCF-7 cells. The conversion and cytotoxicity assays demonstrated the functionality of the yCD in the fusion protein. Similar to the binding assays, the conversion of ^{3}H-5-FC to ^{3}H-5-FU was more efficient in MCF-7 cells compared to T-47D cells as well as at 100 pfu/cell compared to 10 pfu/cell. The conversion at 100 pfu/cell (~200–400 pmol/min/mg) was greater than when pancreatic tumor cells were infected at 25 pfu/cell with bCD (~0.2–0.7 pmol/min/mg) and similar to a catalytically enhanced bCD (~100–250 pmol/min/mg).[12] This catalytically enhanced bCD demonstrated much higher conversion (~1000–2800 pmol/min/mg) when evaluated in human glioma cell lines.[5] Due to the higher expression and conversion in MCF-7 cells compared to T-47D cells, we only

evaluated cytotoxicity in the MCF-7 cells. Interestingly, the IC_{50} after infection at 100 pfu/cell (4.2 μg/ml) was similar to many of the glioma and pancreatic cells infected with the catalytically enhanced bCD, although this construct showed greater ^{3}H-5-FC to ^{3}H-5-FU conversion.[5, 12] This difference is likely due to the inherent sensitivity of the individual cell lines to 5-FU.

In vivo evaluation of AdSSTR2-yCD was then conducted in mice bearing MCF-7 tumor xenografts using conversion assays, biodistribution, and small animal PET imaging. Enzyme activity was confirmed after intratumoral injection of AdSSTR2-yCD by removal of the tumor two days after infection and observing conversion of ^{3}H-5-FC to ^{3}H-5-FU. As expected, more conversion was observed after injection of a higher dose of virus. Previous studies in glioma and pancreatic cancer xenografts using the catalytically enhanced bCD also demonstrated *in vivo* enzyme activity, but 7–20 fold less virus was used in these studies.[5, 12] Biodistribution studies demonstrated a 1.5-fold increase in tumor uptake of ^{64}Cu-CB-TE2A-Y3-TATE after injection of AdSSTR2-yCD compared to saline injected control tumors. This is similar to the 1.7-fold increase observed after injection of AdSSTR2. Interestingly, there was an increase in tumor uptake of ^{64}Cu-CB-TE2A-Y3-TATE in saline injected control mice when compared to mice receiving saline plus an excess of Y3-TATE upon injection of ^{64}Cu-CB-TE2A-Y3-TATE. This indicates SSTR2-receptor specific binding in mice that received saline alone and differs from the *in vitro* results that do not show SSTR2-specific binding in MCF-7 cell without AdSSTR2-yCD or AdSSTR2 infection. This may be due to upregulation of SSTR2 in the tumor xenografts due to exposure to estrogen from the implanted pellets, similar to other studies demonstrating increase in SSTR2 expression after exposure to estrogen.[43, 44] There was a 6.7-fold increase in the tumor uptake of ^{64}Cu-CB-TE2A-Y3-TATE after AdSSTR2-yCD injection compared to the uptake after saline injection plus the blocking agent. Similar to other studies, there was increased liver and spleen accumulation of ^{64}Cu-CB-TE2A-Y3-TATE after injection of AdSSTR2-yCD compared to controls.[15, 45] This is likely due to adenoviral infection of these organs even though the adenovirus was injected intratumorally.[46, 47] MicroPET imaging clearly shows accumulation of ^{64}Cu-CB-TE2A-Y3-TATE in tumors injected with AdSSTR2-yCD (Figure 4 A,C). It is interesting to note the heterogeneity of the radioactive uptake as it is likely that there is preferential uptake of ^{64}Cu-CB-TE2A-Y3-TATE along the injection site of AdSSTR2-yCD, which is similar to previous studies.[17, 45] The SUV analysis shows that there is a 9.6-fold increase in tumor uptake of ^{64}Cu-CB-TE2A-Y3-TATE after AdSSTR2-yCD infection compared to the uptake after saline injection plus the blocking agent. This is similar to the 6.7-fold increase observed in the biodistribution studies. It is not clear why the upregulation of SSTR2 was not observed in this study as there was no difference in the SUV between saline tumors and mice that received saline plus the blocking agent. These studies demonstrate that ^{64}Cu-CB-TE2A-Y3-TATE can be used to non-invasively image the expression of SSTR2-yCD.

In conclusion, we have shown that we can construct an adenovirus containing the SSTR2-yCD fusion protein that it is fully functional. *In vitro* studies demonstrated that the fusion protein can bind a radioactive SSTR2 ligand, convert ^{3}H-5-FC to ^{3}H-5-FU, and be cytotoxic to cells after 5-FC treatment. The activity of the fusion protein was also demonstrated *in*

vivo, and importantly, its expression was capable of being imaged non-invasively using PET. While the use of this model, non-replicative adenovirus vector was sufficient to demonstrate the functionality of the SSTR2-yCD, improved gene delivery vehicles may be needed to optimize its therapeutic utility.

ACKNOWLEDGEMENTS

This work was supported by the Department of Radiation Oncology, Washington University School of Medicine and NIH grant R01 EB004533. The authors gratefully acknowledge Margaret Morris, Nicole Fettig, Lori Strong, and Amanda Roth for performing the small animal imaging studies. Dr. Jeffrey Craft is thanked for his assistance in analysis of the imaging data.

REFERENCES

1. Doloff JC, Waxman DJ. Adenoviral vectors for prodrug activation-based gene therapy for cancer. Anticancer Agents Med Chem. 2014; 14:115–126. [PubMed: 23869779]
2. Lawrence TS, Rehemtulla A, Ng EY, Wilson M, Trosko JE, Stetson PL. Preferential cytotoxicity of cells transduced with cytosine deaminase compared to bystander cells after treatment with 5-flucytosine. Cancer Res. 1998; 58:2588–2593. [PubMed: 9635583]
3. Trinh QT, Austin EA, Murray DM, Knick VC, Huber BE. Enzyme/prodrug gene therapy: Comparison of cytosine deaminase/5-fluorocytosine versus thymidine kinase/ganciclovir enzyme/prodrug systems in a human colorectal carcinoma cell line. Cancer Res. 1995; 55:4808–4812. [PubMed: 7585511]
4. Goblirsch M, Zwolak P, Ramnaraine ML, Pan W, Lynch C, Alaei P, et al. Novel cytosine deaminase fusion gene enhances the effect of radiation on breast cancer in bone by reducing tumor burden, osteolysis, and skeletal fracture. Clin Cancer Res. 2006; 12:3168–3176. [PubMed: 16707617]
5. Kaliberov SA, Markert JM, Gillespie GY, Krendelchtchikova V, Della Manna D, Sellers JC, et al. Mutation of Escherichia coli cytosine deaminase significantly enhances molecular chemotherapy of human glioma. Gene Ther. 2007; 14:1111–1119. [PubMed: 17495948]
6. Kievit E, Bershad E, Ng E, Sethna P, Dev I, Lawrence TS, et al. Superiority of yeast over bacterial cytosine deaminase for enzyme/prodrug gene therapy in colon cancer xenografts. Cancer Res. 1999; 59:1417–1421. [PubMed: 10197605]
7. Liu Y, Ye T, Maynard J, Akbulut H, Deisseroth A. Engineering conditionally replication-competent adenoviral vectors carrying the cytosine deaminase gene increases the infectivity and therapeutic effect for breast cancer gene therapy. Cancer Gene Ther. 2006; 13:346–356. [PubMed: 16179927]
8. Miller CR, Williams CR, Buchsbaum DJ, Gillespie GY. Intratumoral 5-fluorouracil produced by cytosine deaminase/5-fluorocytosine gene therapy is effective for experimental human glioblastomas. Cancer Res. 2001; 62:773–780. [PubMed: 11830532]
9. Russell PJ, Kharti A. Novel gene-directed enzyme prodrug therapies against prostate cancer. Expert Opin Investig Drugs. 2006; 15:947–961.
10. Stackhouse MA, Pederson LC, Grizzle WE, Curiel DT, Gebert J, Haack K, et al. Fractionated radiation therapy in combination with adenoviral delivery of the cytosine deaminase gene and 5-fluorocytosine enhances cytotoxic and antitumor effects in human colorectal and cholangiocarcinoma models. Gene Ther. 2000; 7:1019–1026. [PubMed: 10871750]
11. Kong H, Tao L, Qi K, Wang Y, Li Q, Du J, et al. Thymidine kinase/ganciclovir and cytosine deaminase/5-fluorocytosine suicide gene therapy-induced cell apoptosis in breast cancer cells. Oncol Rep. 2013; 30:1209–1214. [PubMed: 23799574]
12. Kaliberova LN, Della Manna DL, Krendelchtchikova V, Black ME, Buchsbaum DJ, Kaliberov SA. Molecular chemotherapy of pancreatic cancer using novel mutant bacterial cytosine deaminase gene. Mol Cancer Ther. 2008; 7:2845–2854. [PubMed: 18790765]
13. Stolworthy TS, Korkegian AM, Willmon CL, Ardiani A, Cundiff J, Stoddard BL, et al. Yeast cytosine deaminase mutants with increased thermostability impart sensitivity to 5-fluorocytosine. J Mol Biol. 2008; 377:854–869. [PubMed: 18291415]

14. Johnson AJ, Ardiani A, Sanchez-Bonilla M, Black ME. Comparative analysis of enzyme and pathway engineering strategies for 5FC-mediated suicide gene therapy applications. Cancer Gene Ther. 2011; 18:533–542. [PubMed: 21394105]
15. Rogers BE, Parry JJ, Andrews R, Cordopatis P, Nock BA, Maina T. MicroPET imaging of gene transfer with a somatostatin receptor-based reporter gene and ^{94m}Tc-demotate 1. J Nucl Med. 2005; 46:1889–1897. [PubMed: 16269604]
16. Rogers BE, Zinn KR, Buchsbaum DJ. Gene transfer strategies for improving radiolabeled peptide imaging and therapy. Q J Nucl Med. 2000; 44:208–223. [PubMed: 11105586]
17. Zinn KR, Buchsbaum DJ, Chaudhuri T, Mountz JM, Kirkman RL, Rogers BE. Noninvasive monitoring of gene transfer using a reporter receptor imaged with a high affinity peptide radiolabeled with ^{99m}Tc or ^{188}Re. J Nucl Med. 2000; 41:887–895. [PubMed: 10809205]
18. Zinn KR, Chaudhuri TR. The type 2 human somatostatin receptor as a platform for reporter gene imaging. Eur J Nucl Med. 2002; 29:388–399.
19. Dmitriev IP, Kashentseva EA, Kim KH, Matthews QL, Krieger SS, Parry JJ, et al. Monitoring of biodistribution and persistence of conditionally replicative adenovirus in a murine model of ovarian cancer using capsid-incorporated mCherry and expression of human somatostatin receptor subtype 2. Mol Imaging. 2014; 13
20. Weckbecker G, Lewis I, Albert R, Schmid HA, Hoyer D, Bruns C. Opportunities in somatostatin research: biological, chemical, and therapeutic aspects. Nat Rev Drug Discov. 2003; 2:999–1017. [PubMed: 14654798]
21. Rogers BE, Chaudhuri TR, Reynolds PN, Della Manna D, Zinn KR. Non-invasive gamma camera imaging of gene transfer using an adenoviral vector encoding an epitope tagged receptor as a reporter. Gene Ther. 2003; 10:105–114. [PubMed: 12571639]
22. Rogers BE, McLean SF, Kirkman RL, Della Manna D, Bright SJ, Olsen CC, et al. In vivo localization of [^{111}In]-DTPA-d-Phe^{1}-octreotide to human ovarian tumor xenografts induced to express the somatostatin receptor subtype 2 using an adenoviral vector. Clin Cancer Res. 1999; 5:383–393. [PubMed: 10037188]
23. Achilefu S, Wilhelm RR, Jimenez HN, Schmidt MA, Srinivasan A. A new method for the synthesis of tri-tert-butyl diethylenetriaminepentaacetic acid and its derivatives. J Org Chem. 2000; 65:1562–1565. [PubMed: 10814125]
24. Weisman GR, Wong EH, Hill DC, Rogers ME, Reed DP, Calabrese JC. Synthesis and Transition Metal Complexes of New Cross-Bridged Tetraamine Ligands. J Chem Soc, Chem Commun. 1996:947–948.
25. Sprague JE, Peng Y, Sun X, Weisman GR, Wong EH, Achilefu S, et al. Preparation and biological evaluation of copper-64-labeled Tyr^{3}-octreotate using a cross-bridged macrocyclic chelator. Clin Cancer Res. 2004; 10:8674–8682. [PubMed: 15623652]
26. Wadas TJ, Anderson CJ. Radiolabeling of TETA- and CB-TE2A-conjugated peptides with copper-64. Nat Protoc. 2007; 1:3062–3068. [PubMed: 17406569]
27. Hatzoglou A, Ouafik L, Bakogeorgou E, Thermos K, Castanas E. Morphine cross-reacts with somatostatin receptor SSTR2 in the T47D human breast cancer cell line and decreases cell growth. Cancer Res. 1995; 55:5632–5636. [PubMed: 7585646]
28. Kharmate G, Rajput PS, Lin YC, Kumar U. Inhibition of tumor promoting signals by activation of SSTR2 and opioid receptors in human breast cancer cells. Cancer Cell Int. 2013; 13:93. [PubMed: 24059654]
29. Smith-Jones PM, Bischof C, Leimer M, Gludovacz D, Angelberger P, Pangerl T, et al. DOTA-lanreotide: a novel somatostatin analog for tumor diagnosis and therapy. Endocrinology. 1999; 140:5136–5148. [PubMed: 10537142]
30. Takahashi M, Valdes G, Hiraoka K, Inagaki A, Kamijima S, Micewicz E, et al. Radiosensitization of gliomas by intracellular generation of 5-fluorouracil potentiates prodrug activator gene therapy with a retroviral replicating vector. Cancer Gene Ther. 2014; 21:405–410. [PubMed: 25301172]
31. Zhang J, Kale V, Chen M. Gene-directed enzyme prodrug therapy. AAPS J. 2015; 17:102–110. [PubMed: 25338741]
32. Adachi Y, Tamiya T, Ichikawa T, Terada K, Ono Y, Matsumoto K, et al. Experimental gene therapy for brain tumors using adenovirus-mediated transfer of cytosine deaminase gene and uracil

phosphoribosyltransferase gene with 5-fluorocytosine. Hum Gene Ther. 2000; 11:77–89. [PubMed: 10646641]

33. Altaner C, Altanerova V, Cihova M, Ondicova K, Rychly B, Baciak L, et al. Complete regression of glioblastoma by mesenchymal stem cells mediated prodrug gene therapy simulating clinical therapeutic scenario. Int J Cancer. 2014; 134:1458–1465. [PubMed: 24038033]
34. Aboagye EO, Artemov D, Senter PD, Bhujwalla ZM. Intratumoral conversion of 5-fluorocytosine to 5-fluorouracil by monoclonal antibody-cytosine deaminase conjugates: Noninvasive detection of prodrug activation by magnetic resonance spectroscopy and spectroscopic imaging. Cancer Res. 1998; 58:4075–4078. [PubMed: 9751613]
35. Gade TP, Koutcher JA, Spees WM, Beattie BJ, Ponomarev V, Doubrovin M, et al. Imaging transgene activity in vivo. Cancer Res. 2008; 68:2878–2884. [PubMed: 18413756]
36. Hamstra DA, Lee KC, Tychewicz JM, Schepkin VD, Moffat BA, Chen M, et al. The use of ^{19}F spectroscopy and diffusion-weighted MRI to evaluate differences in gene-dependent enzyme prodrug therapies. Mol Ther. 2004; 10:916–928. [PubMed: 15509509]
37. Li C, Penet MF, Wildes F, Takagi T, Chen Z, Winnard PT, et al. Nanoplex delivery of siRNA and prodrug enzyme for multimodality image-guided molecular pathway targeted cancer therapy. ACS Nano. 2010; 4:6707–6716. [PubMed: 20958072]
38. Freytag SO, Barton KN, Brown SL, Narra V, Zhang Y, Tyson D, et al. Replication-competent adenovirus-mediated suicide gene therapy with radiation in a preclinical model of pancreatic cancer. Mol Ther. 2007; 15:1600–1606. [PubMed: 17551507]
39. Freytag SO, Khil M, Stricker H, Peabody J, Menon M, DePeralta-Venturina M, et al. Phase I study of replication-competent adenovirus-mediated double suicide gene therapy for the treatment of locally recurrent prostate cancer. Cancer Res. 2002; 62:4968–4976. [PubMed: 12208748]
40. Hackman T, Doubrovin M, Balatoni J, Beresten T, Ponomarev V, Beattie B, et al. Imaging expression of cytosine deaminase-herpes virus thymidine kinase fusion gene (CD/TK) expression with [^{124}I]FIAU and PET. Mol Imaging. 2002; 1:36–42. [PubMed: 12920859]
41. Xia K, Liang D, Tang A, Feng Y, Zhang J, Pan Q, et al. A novel fusion suicide gene yeast CDglyTK plays a role in radio-gene therapy of nasopharyngeal carcinoma. Cancer Gene Ther. 2004; 11:790–796. [PubMed: 15499380]
42. Zinn KR, Chaudhuri TR, Krasnykh VN, Buchsbaum DJ, Belousova N, Grizzle WE, et al. Gamma camera dual imaging with a somatostatin receptor and thymidine kinase after gene transfer with a bicistronic adenovirus in mice. Radiology. 2002; 223:417–425. [PubMed: 11997547]
43. Rivera JA, Alturaihi H, Kumar U. Differential regulation of somatostatin receptors 1 and 2 mRNA and protein expression by tamoxifen and estradiol in breast cancer cells. J Carcinog. 2005; 4:10. [PubMed: 16018813]
44. Xu Y, Song J, Berelowitz M, Bruno JF. Estrogen regulates somatostatin receptor subtype 2 messenger ribonucleic acid expression in human breast cancer cells. Endocrinology. 1996; 137:5634–5640. [PubMed: 8940394]
45. Chen R, Parry JJ, Akers WJ, Berezin MY, El Naqa IM, Achilefu S, et al. Multimodality imaging of gene transfer with a receptor-based reporter gene. J Nucl Med. 2010; 51:1456–1463. [PubMed: 20720053]
46. Lohr F, Huang Q, Hu K, Dewhirst MW, Li CY. Systemic vector leakage and transgene expression by intratumorally injected recombinant adenovirus vectors. Clin Cancer Res. 2001; 7:3625–3628. [PubMed: 11705885]
47. Wang Y, Hu JK, Krol A, Li YP, Li CY, Yuan F. Systemic dissemination of viral vectors during intratumoral injection. Mol Cancer Ther. 2003; 2:1233–1242. [PubMed: 14617797]

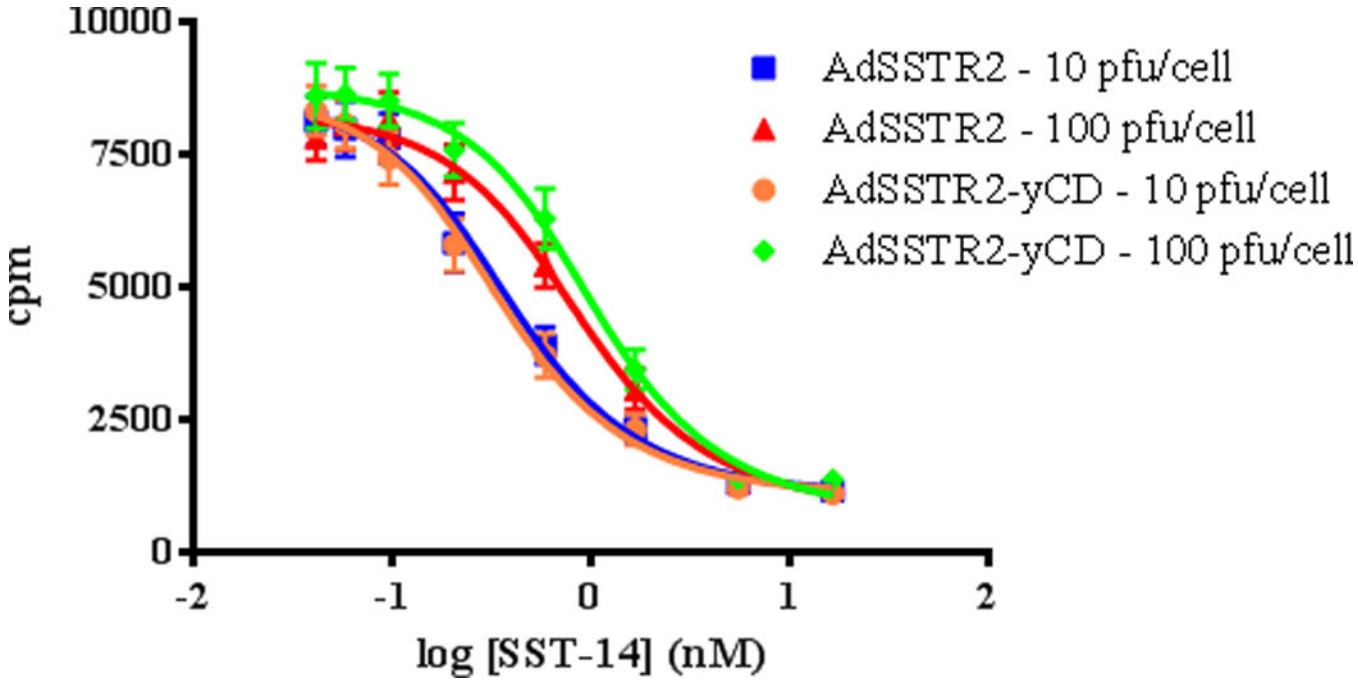

Figure 1.

Representative competitive binding assay curves on MCF-7 cells infected with either AdSSTR2 or AdSSTR2-yCD at 10 or 100 pfu/cell. The data were generated using GraphPad Prism 4 from triplicate cpm measurements for each concentration of ligand.

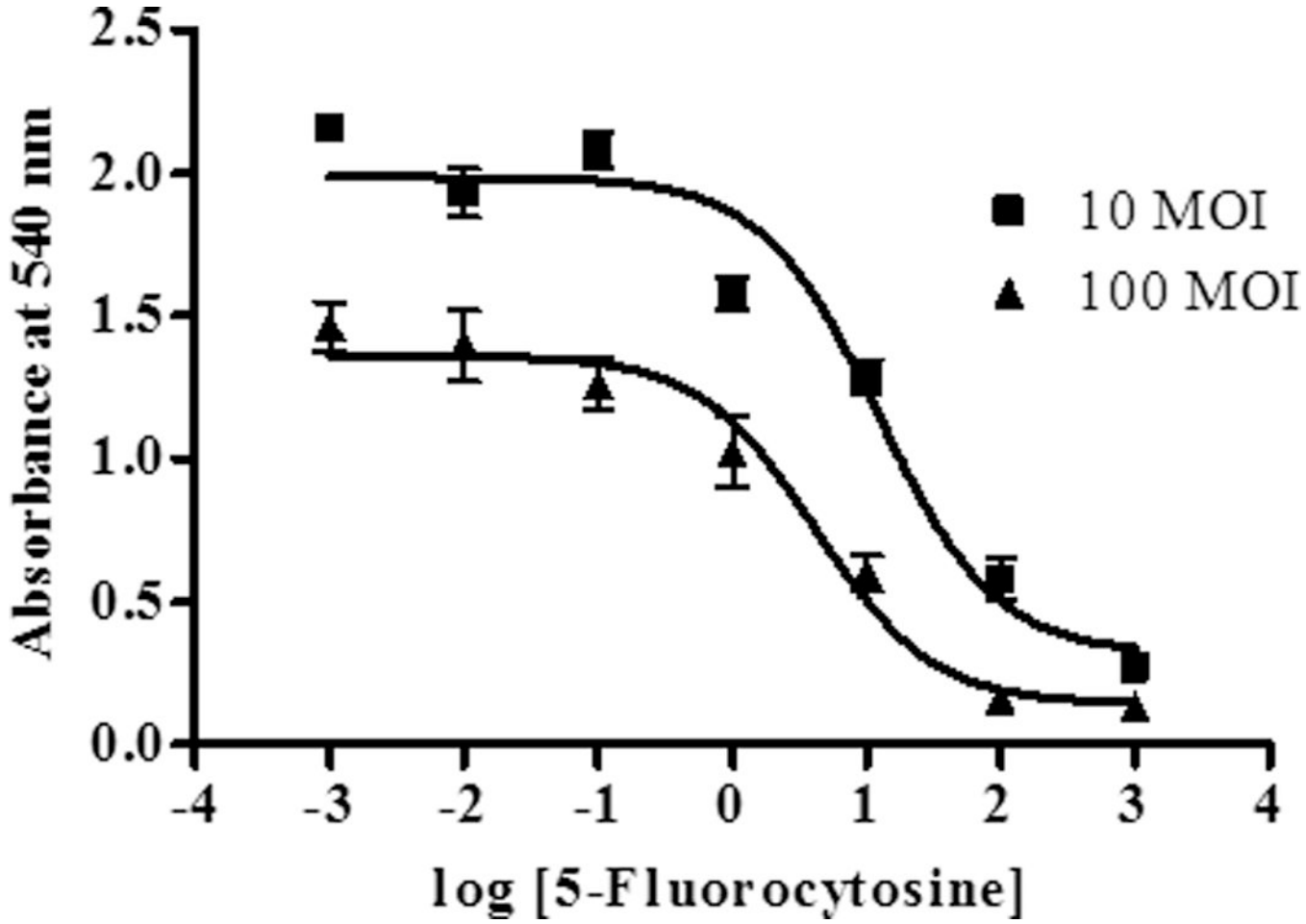

Figure 2.

Cell anti-proliferation data from MCF-7 cells infected with AdSSTR2-yCD at 10 or 100 pfu/cell. The data were generated using GraphPad Prism 4 from triplicate absorbance measurements for each concentration of ligand in which viable cells were fixed and stained with 2% crystal violet in 70% ethanol. The fixed cells were then washed, dried, and the absorbance was measured. The graph is a representative IC_{50} curve, with each point being a triplicate measurement. The IC_{50} (μg/mL) values are the mean ± SEM of three experiments, each performed in triplicate.

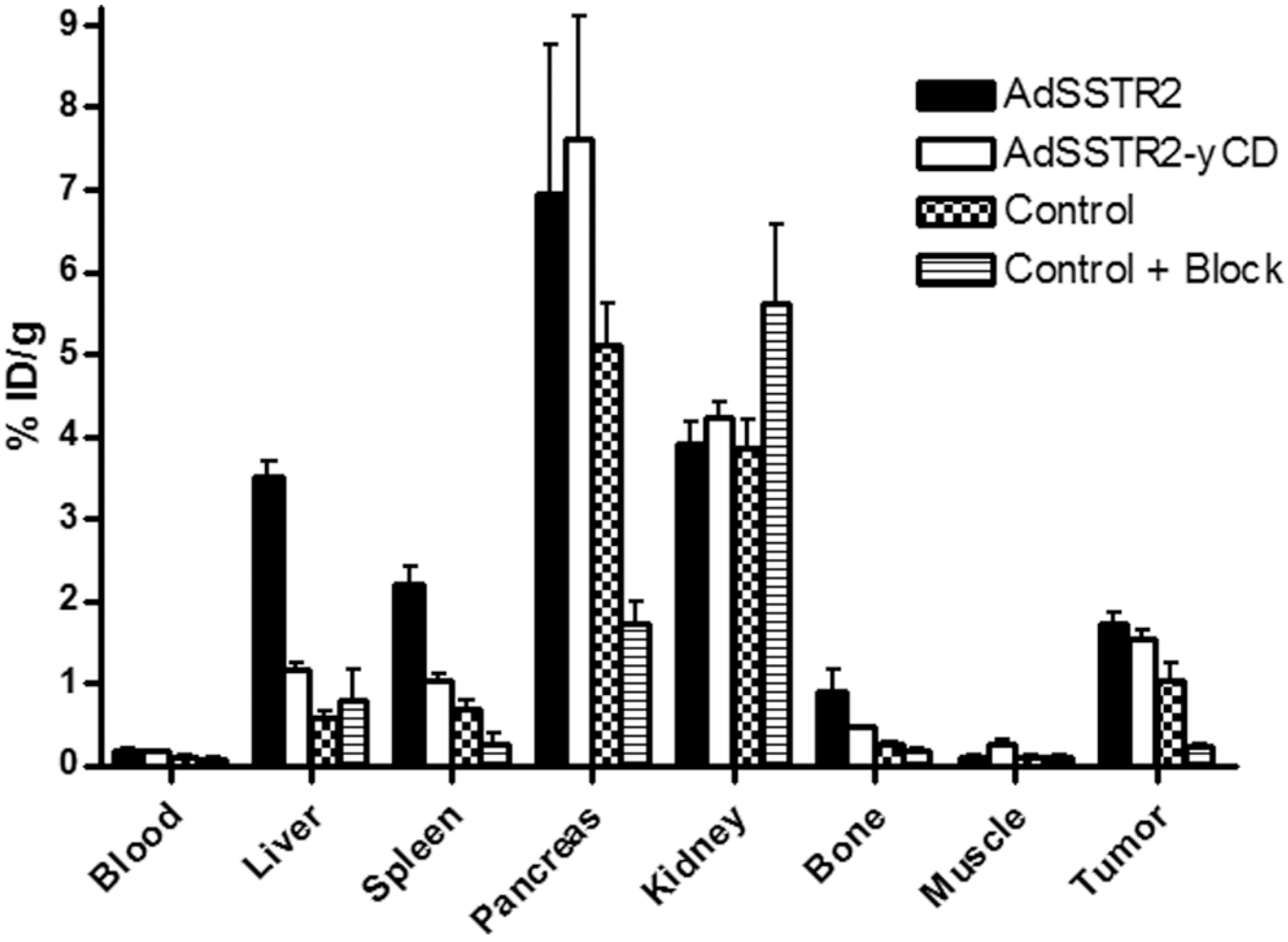

Figure 3.

Biodistribution of ^{64}Cu-CB-TE2A-Y3-TATE in female CB.17 SCID mice implanted with MCF-7 xenografts on the rear flank. The tumors were allowed to grow with 17β-estradiol supplementation, followed by intratumoral injection of AdSSTR2 or AdSSTR2-yCD. Control mice received an intratumoral injection of saline. Two days later, ^{64}Cu-CB-TE2A-Y3-TATE was injected intravenously into each mouse. The mice were sacrificed 4 h post-injection, and the tissues were removed to determine radioactive content. Another control group received the intratumoral saline injection followed by co-injection of ^{64}Cu-CB-TE2A-Y3-TATE and 200 μg of Y3-TATE as a blocking agent. The data represent the mean ± SEM of the % injected dose per gram of tissue with n = 3 – 4.

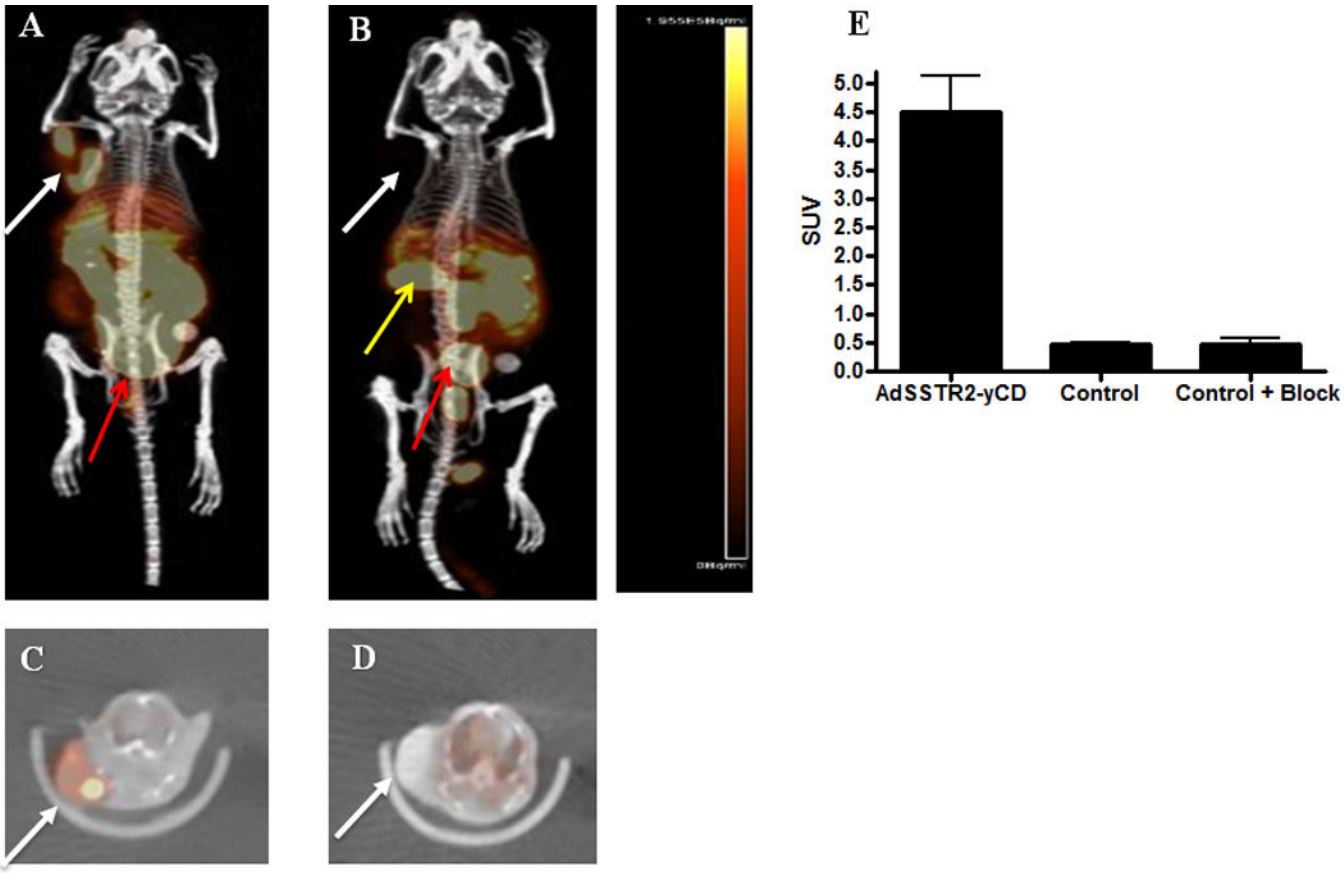

Figure 4.

Representative coronal (A,B) and transaxial (C,D) views of maximum-intensity projections of PET images with co-registered CT of mice bearing MCF-7 tumors at 4 h after injection of ^{64}Cu-CB-TE2A-Y3-TATE. The axillary tumors were injected directly with AdSSTR2-yCD (A,C) or saline (B,D) two days prior to administration of ^{64}Cu-CB-TE2A-Y3-TATE. The images show uptake of ^{64}Cu-CB-TE2A-Y3-TATE in the AdSSTR2-yCD injected tumors, but not the control tumors. The white arrows indicate location of the tumors, the red arrows indicated radioactive excretion through the bladder, and the yellow arrows indicate the location of the kidney. Clearance of ^{64}Cu-CB-TE2A-Y3-TATE through the kidneys is observed in mice where the kidneys are in the field of view (yellow arrows). Panel E shows the SUV analysis for the tumors injected with AdSSTR2-yCD or saline (control). In addition, SUV analysis was performed on a group of mice that received saline followed by co-injection of ^{64}Cu-CB-TE2A-Y3-TATE and 200 μg of Y3-TATE as a blocking agent (control + block).

Table 1

Binding of ^{125}I-Tyr^{11}-SST-14 to MCF-7 and T-47D cell membranes infected with AdSSTR2-yCD or AdSSTR2 at 10 or 100 pfu/cell. The binding affinity (K_d) is expressed in pM and the maximum expression (B_{max}) is expressed in fmol/mg.

	AdSSTR2-yCD				AdSSTR2			
	10 pfu/cell		100 pfu/cell		10 pfu/cell		100 pfu/cell	
	K_d	B_{max}	K_d	B_{max}	K_d	B_{max}	K_d	B_{max}
MCF-7	87 ± 23	764 ± 132	200 ± 30	1829 ± 293	80 ± 13	751 ± 107	190 ± 32	1595 ± 157
T-47D	86 ± 47	40 ± 6	134 ± 51	217 ± 25	50 ± 20	32 ± 4	108 ± 53	242 ± 51

Cancer Gene Ther. Author manuscript; available in PMC 2015 October 03.

Table 2

CD conversion activity (pmol/min/mg) of AdSSTR2-yCD in MCF-7 and T-47D cells infected at 10 or 100 pfu/cell (*In Vitro*) or in MCF-7 tumors directly injected with either 1×10^9 or 3×10^9 pfu (*In Vivo*). Conversion activity was not performed (NP) in T-47D tumors *in vivo*.

	In Vitro		***In Vivo***	
	10 pfu/cell	**100 pfu/cell**	**1×10^9 pfu**	**3×10^9 pfu**
MCF-7	62 ± 11	386 ± 27	193 ± 41	698 ± 81
T-47D	11 ± 1	214 ± 58	NP	NP